D. Riveros G., Z. Shokribousjein, P. Losada-Pérez , M. Rheza Khalesi, K. Cordova, C. Michiels, J. A. Delcour, H. Verachtert, P. Wagner and G. Derdelinckx

Comparison of Structure, Sequence, Physical Interactions and its Effects on Primary Gushing among Several Class II Hydrophobins

Class II hydrophobins produced by Ascomycetes exhibit interesting properties as surface active proteins, they are capable of changing the hydropathy of a surface or to behave as an emulsifier due to their globular structure. They are currently known as one the main causes for primary gushing in carbonated beverages by their ability to interact strongly with CO_2 molecules forming nanobubbles. To extend the scope of possibilities for hydrophobin applications four different class II hydrophobins were studied and compared for their ability to adhere to surfaces, their surface tension acitivity and ability to interact with CO_2 molecules. By using Quartz crystal microbalance with dissipation monitoring, water contact angle, gushing potential and computer modelization, it is attempted to understand how small differences in their structures and amino acid sequences can lead to differences in physicochemical properties and behavior.

Descriptors: Hydrophobins, self-assembly proteins, gushing

1 Introduction

Hydrophobins are a particular group of proteins produced by filamentous fungi, principally by Ascomycetes and Basidiomycetes, helping fungi to overcome the surface tension of aqueous environments covering the aerial hyphae allowing their aerial growth. Hydrophobins also cover spores during sporulation making them hydrophobic and protecting them against desiccation to improve survival and posterior dissemination [1, 2]. Hydrophobins are divided in two main classes differing in structure and solubility. As a common feature, all hydrophobins share a distinctive set of eight cysteines within their amino acid sequence; these cysteines are responsible for four disuldife brigdes folding the molecule into a globular shape turning hydrophobins very resistant to physical and chemical stresses. Class I has a more disordered conformation but when they assemble together in a monolayer, they form a very rigid structure with rodlet conformation. This conformation can be disrupted only with strong acids like trifluoroacetic acid. On the other hand, class II hydrophobins have a globular shape conformation and are readily soluble in 60 % ethanol [3]. Class II Hydrophobins can form well-ordered monolayers also called self-assembled monolayers (SAM).

Due to their amphiphilic nature hydrophobins tend to migrate to interfaces [4, 5]. Hydrophobins are all surface active molecules from monomers to multimers [6] and this characteristic allows them to form well-ordered monolayers as well as bilayers [7–9] when they interact in solution and with surfaces. Currently a significant amount of research concerns the use of hydrophobins for emulsification processes [10] and their use as nanocarriers for drug compounds and other medicinal substances as well as for food additives [11–13].

Class II hydrophobins are however also involved on a physical phenomenon observed with carbonated beverages known as primary gushing which is the spontaneous overfoaming of a liquid after opening a closed bottle without any external energy input. This is due to the interaction of these proteins with carbon dioxide molecules in the bottles forming semi rigid structures of protein with CO_2 resembling small nanobubbles. When a container (bottle) is opened the sudden change in pressure creates spontaneous energy liberation and many nucleation sites leading to gushing. Further details about this process can be found elsewhere [14, 15]. Class II hydrophobins HFBI and HFBII have been well characterized, their structure has been determined by X-ray crystallography and many of their interfacial and rheological properties have been characterized [16–24]. However, HFBI and HFBII cannot represent the entire group of class II hydrophobins. it has been noticed that within them are differences in amino acid sequence, structural folding and protein-protein interactions which finally lead to different behavior in adsorption to surfaces, surface tension activity and interaction with gaseous molecules in carbonated beverages

Authors

Msc. David Santiago Riveros Galan, Dr. Zahra Shokribousjein, Msc. Karla Cordova Aguilar, Prof. Dr. Chris Michiels, Prof. Dr. Ir. Jan Delcour, Prof. Dr. Ir. Hubert Verachter, Prof. Dr. Ir. Guy Derdelinckx, KULeuven, Department of Microbial and Molecular Systems (M2S), and Leuven Food Science and Nutrition Research Centre (LFoRCE-MaltBeerSci), Heverlee, Belgium; Dr. Patricia Losada Perez, Instituut voor Materiaal onderzoek, Campus Diepenbeek, Diepenbeek, Hasselt, Belgium; Dr. Mohammad Rheza Khalesi, Prof. Dr. Ir. Patrick Wagner; corresponding author: DavidSantiago.RiverosGalan@biw.kuleuven.be

as it has been noticed by other researchers, e.g. Sarlin (2012) who found that using different class II hydrophobins the degree of overfoaming varied suggesting that every hydrophobin has a different degree of interaction with CO_2.

To get a better insight of the relation between class II hydrophobin structures and interfacial and physicochemical properties this research focused on studying the structural differences of four different class II hydrophobins HFBI, HFBII from *Trichoderma reesei*; HFB2-a2 from *Trichoderma Harzianum* [25] and Fghyd5 from *Fusarium graminearum*. Molecular modeling comparison and protein self-association simulation was studied using rosetta docking server and PYMOL software, along with the determination of physicochemical properties like adsorption ability to different surfaces, surface tension decreasing, and water contact angle. This research aims to gain more insight into the mechanisms controlling the self-assembly of these proteins and their surface properties. Understanding of these mechanisms will be a valuable tool for expanding the range of possibilities for applications of hydrophobins on industry and scientific research.

2 Materials and methods

2.1 Fungal strains and cultivation methods

For hydrophobin production three different strains were used: *Trichoderma reesei* MUCL 44908, *Trichoderma harzianum* and *Fusarium graminearum* strains, which were kindly provided by Prof. Bruno Cammue (Centre of Microbial and Plant Genetics, KULeuven). All the strains were maintained on PDA petri plates at 25°C. Hydrophobin HFBI and the hydrophobin from *Trichoderma harzianum* were produced in liquid media containing glucose 40 g/L, peptone 5 g/L, yeast extract 1.25 g/L, KH_2PO_4 5 g/L, $(NH_4)_2SO_4$ 3.5 g/L, $MgSO_4 \cdot 7H_2O$ 0.75 g/L, $CaCL_2$ 0.75 g/L, $CoCL_2 \cdot 6H_2O$ 40 mg/L, $MnSO_4 \cdot H_2O$ 32 mg/L, $ZnSO_4 7H_2O$ 10 mg/L (9) with a pH adjusted to 5. For HFBII a medium with the same components was used, except for glucose, which was substituted by lactose (40g/L)For the *Fusarium graminearum* hydrophobin FgHYD5 potato dextrose broth (PDB) containing glucose 20 g/L and, potato extract 4 g/L was used. The fungi were cultivated in conical flasks for 5 days at 25 °C on a rotary shaker at 200 rpm.

2. 2 Hydrophobin purification

Hydrophobin HFBII was extracted following the method of [26]. The other hydrophobins (HFBI, HFB2-a2 and FgHYD5) were isolated as follows: The liquid culture was filtered through a cheese cloth and all the biomass was collected and resuspended in a 60 % ethanol solution (about three times the amount of mass collected) during 1 hour with periodical shaking, after that, the samples were centrifuged and the supernatant was collected. The protein extracts were further purified by chromatography using a reverse phase chromatography RPC column (6.4×100 mm; GE Healthcare) and a gradient elution from 0.1 % TFA in MilliQ water (A) to 0.1 % TFA in acetonitrile (B). The subsequent eluate was monitored by UV detection at 214 nm. Positive fractions containing purified hydrophobins (fractions between 40–50 % of acetonitrile) were collected. All collected (hydrophobin) fractions were confirmed by matrix laser desorption ionization time of flight (MALDI-TOF) mass spectrometry using an Ultraflex II instrument (Brüker Daltonics, GmbH) in linear mode with α-cyano-4-hydroxy cinnamic acid as matrix. Once confirmed and purified, the samples were freeze dried and resolubilized in distilled water for further experiments. The amount of protein present in the samples was determined using Nanodrop (Thermo Scientific) where the amount of protein is calculated using the absorbance measurements at 280 nm compared to a blank (water in our case) following the beer-lambert equation to calculate the concentration of the measured protein.

$$Absorbance = -\log \frac{\text{Intensity } sample}{\text{Intensity } blank}$$

2.3 Gushing analysis

For gushing tests, bottles with 7 g/L CO_2 were supplemented separately with known concentrations of purified hydrophobins, at 4 °C, to avoid CO_2 losses during the opening of the bottle. Once the bottles were again tightly closed and turned gently several times to ensure correct mixing, then they were placed on a horizontal shaker (Buhler SM30, Germany) at 150 rpm during 3 days at 25 °C. After that, the bottles were left to rest for 10 minutes, then turned three times with ten seconds intervals between each turning and left for a final rest of 30 seconds before opening. Overfoaming was measured as the difference of weight between the unopened bottle and after opening. Overfoaming larger than 20 ml/L was considered as a gushing positive sample.

2.4 QCM-D measurements

Quartz crystal microbalance with dissipation monitoring (QCM-D) is an acoustic surface-sensitive technique based on the inverse piezoelectric effect. The adsorption ability of hydrophobins was determined using a Q-sense E4 set-up (Q-sense, Gothenborg, Sweden) that measures changes in frequency Δf and dissipation ΔD upon protein adsorption. AT-cut quartz crystals with different coatings (diameter 14 mm, thickness 0.3 mm, surface roughness 3 nm and resonant frequency 4.95 MHz) were used. For hydrophobic adsorption determinations, amorphous fluoropolymer 1600 (Teflon-like) sensors were used. On the other hand, hydrophilic adsorption was monitored onto bare gold-coated sensors. For cleaning, gold-coated sensors were first submerged in a mixture 5:1:1 Milli-Q, ammonia (25 %) and hydrogen peroxide (30 %) at 75 °C for 5 minutes then washed several times with Milli-Q water, finally dried under nitrogen gas and treated under UV/ozone for 10 minutes. Afterwards, they were resubmerged in a solution of 98 % isopropanol at 70 °C for 15 minutes, then rinsed three times with Milli-Q water and finally dried under N_2. Teflon-like sensors were cleaned with 50 % ethanol, rinsed thoroughly with distilled Milli-Q water and finally dried with N_2. The changes in Δf and in ΔD were monitored at five six different overtones (from 1st to 11th, the fundamental frequency is rather unstable since this is the one that reaches the farthest out to the edge of the sensor and may be disturbed by the O-ring).

For every hydrophobin (HFBI, HFBII, HFB2-a2 and FgHYD5) solutions of distilled water with 0.1 mg/ml of protein were used. Measurements were carried out with a continuous flow at a rate

of 50 µL/min, the temperature was kept stable at 18 °C. Acetate buffer was first injected to get a stable baseline and subsequently the protein solution was added.

2.5 Water contact angle determinations

The degree of hydrophilicity was measured with a contact angle analyzer (DataPhysics OCA15 plus device, Germany). Angles were recorded before and after protein adsorption onto the hydrophobic and hydrophilic quartz crystals used on the QCM device. Once the crystals were dried, small drops (2 µL) of Milli-Q® water were gently deposited onto the crystal surface and the drop formed on the surface was analyzed using Kruss image software analyzer, the result was given as the average of several measurements in different parts of the crystal.

2.6 Time dependence of the surface tension by the pendant-drop method

In this method, the surface tension σ (t) was determined according to the shape analysis of a pendant drop based on the Young-Laplace-equation:

$$\Delta P = \sigma\left(\frac{1}{R1}+\frac{1}{R2}\right) \qquad \text{(Eq. 1)}$$

where σ is the surface tension, R1 and R2 are the two principal radii of curvature of the surface, and ΔP is the pressure difference across the interface [27]. Interfacial tension measurements of the tested hydrophobins were performed on using a goniometer (CAM-200, KSV). An air bubble was created with a hook needle using a 10-mL Hamilton syringe in 3 mL of HFBI and HFB-2a-2 solutions with a concentration of 0.2 mg/mL. The change in bubble shape was captured by a FireWire video camera for 601 frames with a frame interval of 5 s. The results were depicted as changes of surface tension and bubble size versus time.

3 Results and Discussion

Structural analysis

The comparison of the amino acid sequence of the four hydrophobins indicated that the configuration of the residues is very similar; the positions of the hydrophobic residues among these four hydrophobins are well conserved (Fig. 1). However, using PYMOL software it was found out that the hydrophobic patch of Fghyd5 is not uniform and it contains hydrophilic spots within the surface. On the other hand, the hydrophobic patch of HFB2-a2 is larger and more uniform than the other three (Fig. 2). It is worth noting that HFB2-a2 exhibits an extra hydrophobic patch located in the hydrophilic part of the protein, giving it additional hydrophobicity and increasing its tendency to migrate to interfaces or interact better with hydrophobic molecules like CO_2. Moreover, the solvent accessible area of the respective hydrophobic patches for these four hydrophobins also exhibited differences. The calculated areas were 21.6 nm² for HFBI, 24.8 nm² for HFBII, 36.6 nm² for HFB2-a2, and 22.8 nm² for FgHYD5. This reflects that the area available for hydrophobic interactions is clearly affected by the way the protein folds.

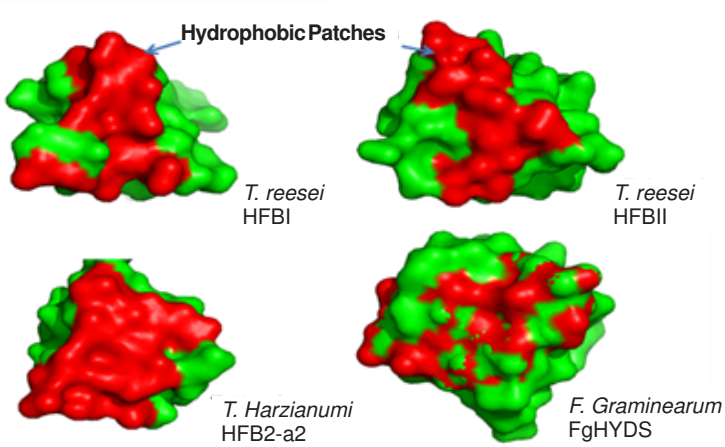

Fig 2. Differences in hydrophobic patches among different hydrophobins used in these research . The models were made using PYMOL. Hydrophobic amino acids from the hydrophobic patch are colored in red

In view of the above results, models of a hydrophobin monolayer were built using 5x4 monomers and then submitted to Rosetta docking server [28–30] to simulate how these proteins interact with other monomers forming then a monolayer. The server de-livered a set of possible interactions. The models with the most stable configuration (lowest free energy) were selected, using PYMOL the hydrophobic patches were colored in order to observe how the hydrophobic patch is exposed after the monolayer formation. It was clear that the hydrophobic area of *Trichoderma harzianum* patch is larger and more uniform than the other three, *Trichoderma reesei* (HFBI and HFBII) exhibit a similar area, however, *Fusarium graminearum* (FgHYD5) showed an irregular hydrophobic patch.

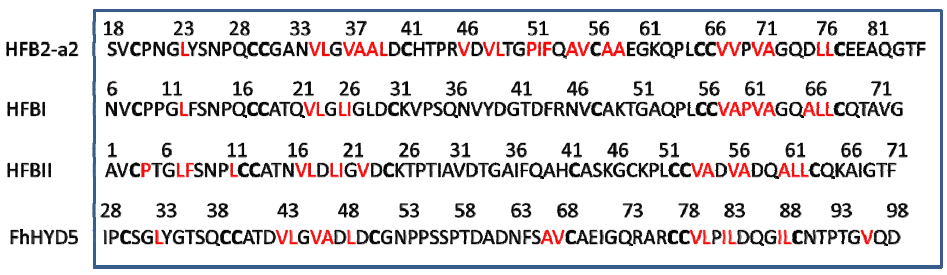

Fig 1. Amino acid sequence of four class II hydrophobins. Hydrophobic amino acids exposed on the surface of the hydrophobic patch are highlighted in red. Orange highlighted residues in HFB2-a2 were founded in the hydrophilic patch of the protein using PYMOL

The monolayer of FgHYD5 exhibited a glutamine residue on position 66 protruding from the surface, decreasing the ability of the hydrophobin to interact strongly with hydrophobic surfaces (Fig. 3A). In the case of HFBI, the hydrophobic patch is more uniform and defined, although a glutamine residue is also present on position 65 protruding beyond the hydrophobic patch. However, the distance is shorter and the arc formed within the hydrophobic patches is smaller than Fghyd5. In the case of HFB2-a2 a highly ordered hydrophobic

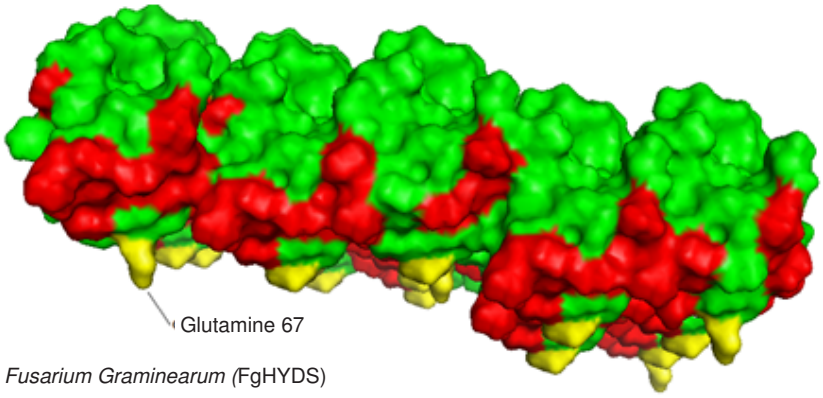

*Fusarium Graminearum (*FgHYDS)

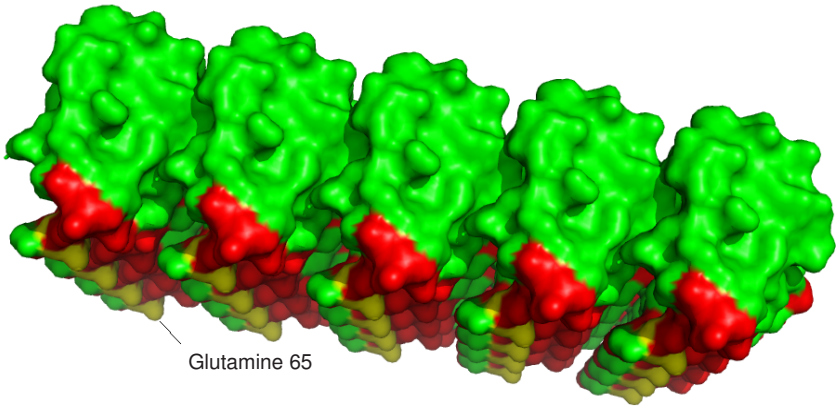

*Trichoderma reesei (*HFBI)

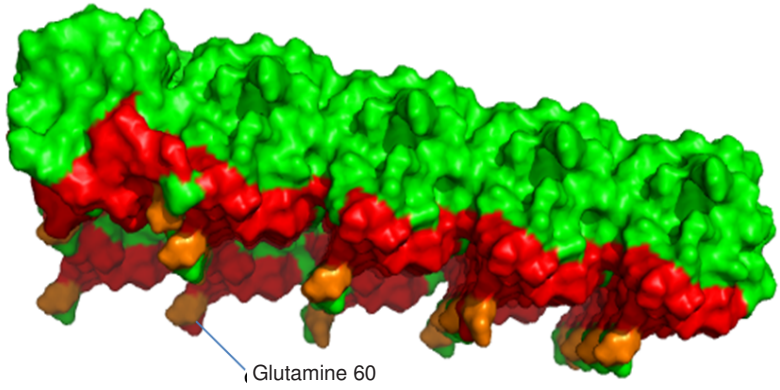

*Trichoderma reesei (*HFBII)

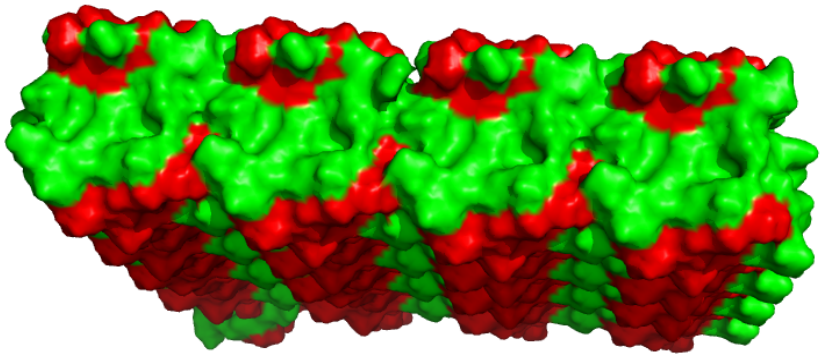

*Trichoderma harzianum (*HFB2-a2)

Fig. 3 Monolayers of three different class II hydrophobins, The hydrophobic patches are colored in red, the yellow areas are glutamine residues among the hydrophobic patch of FgHYD5 and HFBI

patch is shown, with a very well packed conformation. This hydrophobin has a glutamine residue but now on position 68, inside the protein and not present on the hydrophobic patch. It is also noteworthy that the hydrophobic patch of HFB2-a2 is flatter than that of the other three allowing it to interact more strongly with hydrophobic surfaces, as noticed before by other researchers [31].

The interaction with CO_2 molecules, quartz crystal microbalance, water contact angle and pendant drop surface tension were used as an experimental confirmation of the models described above.

3.1 Interaction of hydrophobins with CO_2 gaseous molecules (gushing potentials)

The ability to interact with hydrophobic molecules like CO_2 was measured with different concentrations of hydrophobin and four different class II hydrophobins (Table 1, see page 43).

The gushing potential varied with the type of hydrophobin. At low concentrations HFB2-a2 had a very low threshold to induce overfoaming (3µg/L), while 40µg/L (data not shown) of FgHYD5 was needed to induce a similar amount of overfoaming liquid, which is in agreement with previously reported gushing potential differences in the literature [32]. Differences in the amount of overfoamed liquid may indicate that the interactions with CO_2 molecules are quantitatively different for each type of hydrophobin.

3.2 QCM-D results

The adsorption process observed with quartz crystal microbalance showed that HFBI, HFBII and FgHYD5 share a similar affinity for hydrophobic surfaces, while HFB2-2a showed a stronger adsorption to the hydrophobic surface reaching the highest mass adsorption (Fig. 4, see next page). When hydrophilic surfaces were used, FGHYD5 showed a higher affinity compared to the other hydrophobins. Due to the small changes in dissipation (less than 2 e^{6}) the Sauerbrey equation $\Delta m = -C\,\Delta f\,/n$ was used [33] to calculate the adsorbed mass onto the crystal. Where Δm is the adsorbed mass, n is the overtone or the frequency used to calculate it (n = 3 for 15-Mhz) and C (17.7 ng/cm^2/Hz) is the mass sensivity constant. The third harmonic ($f3$) was used to calculate the adsorbed mass onto the crystals.

Sauerbrey equation was used to calculate the adsorbed mass onto the crystals these masses were plotted in figure 5 (see next page), showing that the mass adsorbed onto the hydrophobic surface was larger for HFB2-a2 than for the other 3. On the other hand, FgHYD5 achieved the highest adsorption onto the hydrophilic surface, this is a logical

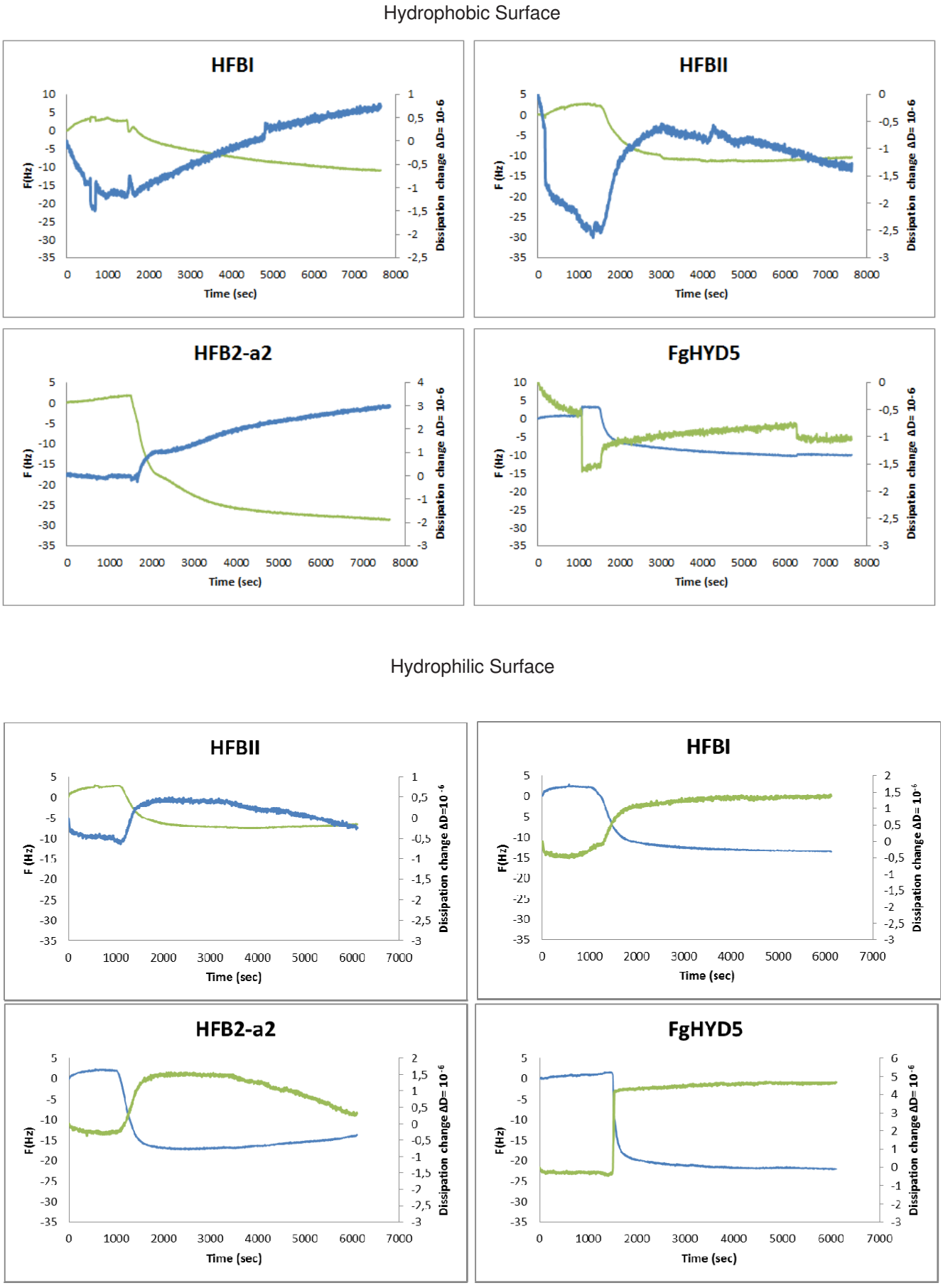

Fig. 4 QCM-D adsortion behavior, blue line: frequency; green line: dissipation

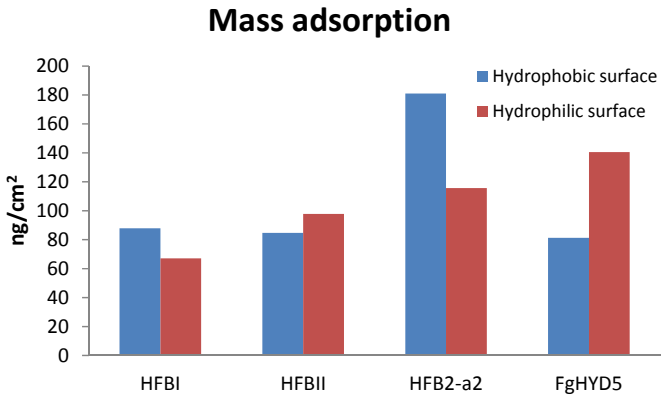

Fig. 5 **Mass adsorption of the four different class II Hydrophobins with hydrophobic (fluoropolymer) and hydrophilic (bare gold) surfaces**

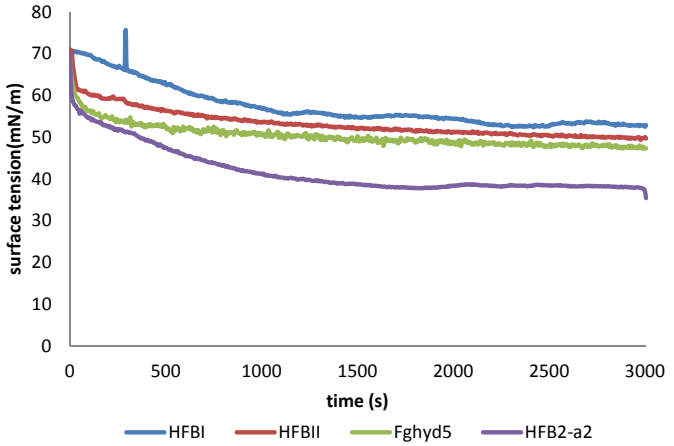

Fig. 6 **Surface tension determination by pendant drop method**

Table 1 **Overfoamings in mL in the gushing tests with different concentrations of purified hydrophobins**

Hydrophobin amount added (ug/L)	Amount of sparkling water gushed (mL) (n = 3)			
	HFBI	**HFBII**	**FgHYD5**	**HFB2-a2**
0.3	0	0	0	0
3	12	15	0	18
30	145	146	0	254
50	191	185	67	270
100	273	260	234	353
150	490	484	352	497
200	516	509	480	562
250	614	614	512	652
300	608	609	548	657

consequence of the frequency change during adsorption experiments.

After hydrophobin adsorption onto hydrophobic and hydrophilic surfaces, the water contact angle was measured. Table 2 indicates that the hydropathy of the tested surface changed after adsorption. With HFB2-a2 the changes in the angles are the largest on both surfaces reaching 37° and 43° on hydrophilic and hydrophobic surfaces respectively. HFBI and HFBII changed the angles in a similar way as HFB2-a2 but changes were less pronounced/significant. For Fghyd5 the changes showed less than 20° difference from the original crystal. These changes confirmed that the protein can adsorb successfully to a surface turning a hydrophilic area into a moderately hydrophobic or viceversa. Looking at the structures in figure 3 the organization and the structure of a hydrophobin monolayer have a definitive effect on the ability to adsorb to different surfaces, as well as on the interaction with other molecules like CO_2.

Surface tension pressure pendant drop

The ability of hydrophobin molecules to adsorb to the gas/water interface was measured by the pendant drop method. The higher the ability to adsorb to an interface, the lower the surface tension is achieved in the gas bubble. The results in figure 6 show that the surface tension for distilled water decreased from 72 mN/M to 38 mN/M with HFB2-a2 and between from 47 to 52 mN/M for HFBI, HFBII and fghyd5. The higher reduction of the surface tension for HFB2-a2 can be related to the presence of a larger hydrophobic patch, which provides this hydrophobin a higher tendency to migrate to an interface. The surface activity of these two hydrophobins was also described before [34–36]. Our results show a similar behavior to the one found for an hydrophobin layer of HFBII using surface pressure and pendant drop technique [37].

4 Conclusions

The structure of four class II hydrophobins was studied and related to their ability to interact with themselves, with other surfaces and with CO_2 molecules. HFB2-a2 from *Trichoderma harzianum* exhibited a stronger tendency to adsorb to hydrophobic interfaces due to its more uniform hydrophobic patch and due to the presence of an additional hydrophobic residue located in the hydrophilic patch. The latter gives the hydrophobin extra hydrophobic area increasing the tendency to migrate to interfaces and to interact more strongly with other hydrophobic surfaces and molecules like CO_2. Structural characterization is consistent with the results obtained by QCM-D and gushing test: HFB2-a2 exhibits the largest adsorbed mass and the largest amount of overfoaming. HFBI and HFBII exhibited a good surface activity though slightly lower than HFB2-2a. Here, we observed that there is a glutamine residue located on the hydrophobic patch that weakens the interaction among molecules and surfaces, thus increasing the distances among them, which diminish the interactions between proteins and surfaces made through Van der Waals forces. FgHYD5 exhibited a lower adsorption to hydrophobic crystals, but a higher affinity to

Table 2 **Water contact angles obtained before and after adsorption in quartz crystal microbalance experiments**

Hydrophobin	hydrophilic crystal		hydrophobic cristal	
	before adsorption	after adsorption	before adsorption	after adsorption
HFBI	15.4 ± 1.1	47 ± 2.3	94.3 ± 1.2	64.3 ± 1.5
HFBII	14.2 ± 1.3	33,8 ± 1.9	90.1 ± 2.3	66.4 ± 2.1
HFB2-2a	17.8 ± 2.1	54 ± 2.4	96.5 ± 0.6	53.2 ± 3.6
FgHYD5	15.5 ± 1.8	28.7 ± 3.5	101.4 ± 3.0	89.3 ± 3.8

hydrophilic surfaces. After modeling of Fghyd5, this hydrophobin showed a less uniform hydrophobic patch, smaller changes in water contact angle and a lower gushing tendency confirming that this hydrophobin interact less strongly with other hydrophobic molecules like CO_2 and hydrophobic surfaces compared with other class II hydrophobins.

In summary, this work provides a more detailed characterization of class II hydrophobins, which, despite the large similarities among them, they exhibit different interfacial behavior. The presence of an extra hydrophobic patch in HFB2-a2 was proven to be a key feature in lowering surface tension and rendering it highly interactive with hydrophobic surfaces and molecules like CO_2. Further studies on this hydrophobin are thus called for and new applications related to its properties may be envisaged.

The authors gratefully acknowledged the support of KULeuven University (Hydrophobin chair) and all his members Breweries Chimay, Duvel-Moorgart, Orval, Rochefort and Malters Cargill, Boortmalt and Dingenmans for his financial and logistic support.

5 References

1. Nakari-Setälä, T.; Aro, N.; Ilmén, M.; Muñoz, G.; Kalkkinen, N. and Penttilä, M: Differential expression of the vegetative and spore bound hydrophobins of *Trichoderma reesei*. Cloning and characterization of the *hfb2* gene Eur, J. Biochem, **248** (1997), pp. 415-423.
2. Askolin, S.; Penttilä, M.; Wösten H. A. B and Nakari Setälä, T.: The Trichoderma reesei hydrophobin genes *hfb1* and *hfb2* have diverse functions in fungal development, FEMS Microbiology letters, **253** (2005), pp. 251-288.
3. Linder, M.; Szilvay R. G.; Nakari Setälä T. and Penttilä E. Merja: Hydrophobins: the protein-amphiphiles of filamentous fungi, FEMS Microbiology reviews, **29** (2005), pp. 877-896.
4. Szilvay (a), G.; Paananen, A.; Laurikainen, K.; Vuorimaa, E.; Lemmetyinen, H.; Peltonen, J. and Linder, M. B: Self-Assembled Hydrophobin Protein Films at the Air-Water Interface: Structural Analysis and Molecular Engineering, Biochemistry, **46** (2007), pp. 2345-2354.
5. Szilvay (b), G. R.; Kisko, K.; Serimaa, R. and Linder, M. B.: The relation between solution association and surface activity of the hydrophobin HFBI from *Trichoderma reesei*. FEBS Lett. **581** (2007), pp. 2721-2726.
6. Kisko, K.: Characterization Of Hydrophobin Proteins at Interfaces and in Solutions Using X Rays, Academic Dissertation, University of Helsinki, Faculty of Science, Department of Physics, 2008.
7. Lumdson, S. O.; Green, J. and Stieglitz, B.: Adsorption of hydrophobin proteins at hydrophobic and hydrophilic interfaces. Colloids Surf. B Biointerf. **44** (2005), pp. 172-178.
8. Basheva (b), E. S.; Kralchevsky, P. A; Christov, N. C.; Danov, K. D.; Stoyanov, S. D.; Blijdenstein, T. B. J.; Hyung-Jung, K.; Pelan E. G. and Lips, A.: Unique Properties of Bubbles and Foam Films Stabilized by HFBII Hydrophobin, Langmuir. (2011), pp. 2382-2392.
9. Basheva, E. S.; Kralchevsky, P. A.; Danov, K. D.; Stoyanov, S. D.; Blijdenstein, T. B. J.; Pelan, E. G. and Lips, A.: Self-assembled bilayers from the protein HFBII hydrophobin: nature of the adhesion energy. Langmuir, **27** (2011), no. 10, pp. 4481-4488.
10. Green,J. A.; Littlejohn K. A.; Hooley P. and Cox W. P.: Formation and stability of food foams and aerated emulsions: hydrophobins as novel functional ingredients, Current opinion in colloid and interface science, **18** (2013), no. 4, pp. 292-301.
11. Haas, M.; Akanbi, J.; Post, E.; Meter-Arkema, A.; Rink, R.; Robillard, G. T.; Wang, X.; Wösten, H. A. B. and Scholtmeijer K.: Use of hydrophobins in formulation of water insoluble drugs for oral administration, Colloids and surfaces B: Biointerfaces. **75** (2010), pp. 526-531.
12. Cox, A. R.; Aldred, D. and Russell, A.: Exceptional stability of food foams using class II hydrophobin HFBII, Food hydrocolloids, **23** (2009), pp. 366-376.
13. Dickinson, E.: Food emulsions and foams: stabilization by particles, Current opinion in colloid and interfacial science, **15** (2010), pp. 40-49.
14. Sarlin, T.: Detection and characterization of Fusarium hydrophobins inducing gushing in beer, Thesis dissertation,VTT, Finland, 2012.
15. Deckers, S.: Modeling and biophysical characterization of the primary gushing in beer, Thesis dissertation, KULeuven, Heverlee, Belgium, 2013.
16. Askolin, S. Characterization of the Trichoderma reesei Hydrophobins HFBI and HFBII. Dissertation for the degree of Doctor of Science in Technology, VTT publications, Finland, 2006.
17. Bettini, P. P.; Frascella, A.; Comparini, C.; Carresi, L.; Pepori, A. L.; Pazzagli, L.; Cappugi, G.; Scala, F. and Scala, A.: Identification and characterization of GEO1, a new class II hydrophobin from Geosmithia spp. Can J Microbiol. **58** (2002), no. 8, pp. 965-972.
18. De Vries, O. M.; Moore, S.; Arntz, C.; Wessels, J. G. and Tudzynski, P.: Identification and characterization of a tri-partite hydrophobin from Claviceps fusiformis. A novel type of class II hydrophobin. Eur J Biochem. **262**, (1999), no. 2, pp.377-385.
19. Hakanpaa, J.; Linder, M.; Popov, A.; Schmidt, A. and Rouvinen, J.: Hydrophobin HFBII in detail: ultrahigh-resolution structure at 0.75 Å. Acta Crystallogr. Sect.D. **62** (2006), pp. 356-367
20. Hakanpaa, J.; Paananen, A.; Askolin, S.; Nakari-Setala, T.; Parkkinen, T.; Penttila, M.; Linder, M. B. and Rouvinen, J.: Atomic resolution structure of the HFBII hydrophobin, a self-assembling amphiphile. J.Biol.Chem. **279** (2004), pp. 534-539.
21. Johansson, H.: Extraction and characterization of hydrophobins from Trichoderma reesei. Degree project work, Linnaeus University, Kalmer, Sweden, 2010.
22. Kallio, J. M.; Linder, M. B. and Rouvinen, J.: Crystal Structures of Hydrophobin HFBII in the Presence of Detergent Implicate the Formation of Fibrils and Monolayer Films. J. Biol. Chem. **282** (2007), no. 39, pp. 28733-28739.
23. Kwan, A. H.; Winefield, R. D.; Sunde, M.; Matthews, J. M.; Haverkamp, R. G.; Templeton, M.D. and Mackay, J.P.: Structural basis for rodlet assembly in fungal hydrophobins. Proc.Natl.Acad.Sci.Usa. **106** (2006), pp. 3621-3626.
24. Morris, V. K.; Kwan, A. H. and Sunde, M.: Analysis of the structure and conformational states of DewA gives insight into the assembly of the fungal hydrophobins. J. Mol. Biol. **427** (2012), no. 6 pp. 83-86.
25. Mikus, M.; Hatvani, L.; Neuhof, T.; Komoń-Zelazowska, M.; Dieckmann, R.; Schwecke, T.; Druzhinina, I. S.; von Döhren, H. and Kubicek, C. P.: Differential Regulation and Posttranslational Processing of the Class II Hydrophobin Genes from the Biocontrol Fungus *Hypocrea atroviridis*. Appl Environ Microbiol. **75** (2009), no. 10, pp. 3222-3229.
26. Deckers, S. M.; Lorgouilloux, Y.; Gebruers, K.; Baggerman, G. A.; Michiels, C.; Verachtert, H.; Neven, H.; Derdelinckx, G.; Delcour, J. A. and Martens, J.: Dynamic light scattering (DLS) as a tool to detect CO_2-hydrophobin structures and study the primary gushing potential of beer. J. Am. Soc. Brew. Chem. **69** (2012), no. 3, pp. 144-149.

27. Tamm, F.; Sauer, G.; Scampicchio, M. and Drusch, S.: Pendant drop tensiometry for the evaluation of the foaming properties of milk-derived proteins. Food Hydrocolloids. **27** (2012), pp. 371-377.
28. Lyskov S. and Gray J. J.: The Rosetta Dock server for local protein-protein docking. Nucleic Acids Research **36** (Web Server Issue), W233-W238 (2008).
29. Chaudhury S; Berrondo M; Weitzner B. D.; Muthu P.; Bergman H. and Gray J. J.: Benchmarking and analysis of protein docking performance in Rosetta v3.2.PLoS One. **6** (2011), no. 8, p. 22477
30. Lyskov S.; Chou F. C.; Conchúir, S. Ó.; Der B. S.; Drew, K.; Kuroda, D.; Xu, J.; Weitzner B. D.; Renfrew P. D.; Sripakdeevong P.; Borgo B.; Havranek J. J.; Kuhlman B.; Kortemme T.; Bonneau R.; Gray J. J. and Das, R.: Serverification of Molecular Modeling Applications: The Rosetta Online Server That Includes Everyone (ROSIE). PLoS One. **22** (2013) no. 5 May, p. e63906.
31. Shokribousjein, Z.; Riveros, D.; Losada-Pérez, P.; Pepicelli, M.; Gupta, M.; Khalesi, M.; Michiels, C.; Delcour, J. A.; Verachtert, H.; De Maeyer, M.; Wagner, P.; Peeters, C.; Vermant, J. and Derdelinckx, G.: Comparison of structure and properties of two class II hydrophobin HFB-2a-2 from Trichoderma harzianum and HFBI from Trichoderma reesei. 2014. In submission.
32. Sarlin, T; Nakari-Setälä, T.; Linder, M.; Penttilä, M. and Haikara, A.: Fungal hydrophobins as predictors of the gushing activity in malt. J. Inst. Brew. **111** (2002), no. 2, pp. 105-111.
33. Sauerbrey, G.: Verwendung von Schwingquarzen zur Wägung dünner Schichten und zur Mikrowägung. Zeitschrift für Physik. **155** (1959), no. 2, April, pp. 206-222.
34. Jönsson, B.; Lindman, B.; Holmberg, K. and Kronberg, B.: Surfactants and Polymers in Aqueous Solution. John Wiley & Sons, Chichester. 1998, p. 438.
35. van Wetter, M. A.; Wösten, H. A. and Wessels, J. G.: SC3 and SC4 hydrophobins have distinct roles in formation of aerial structures in dikaryons of Schizophyllum commune. Mol. Microbiol. **36** (2000), pp. 201-210.
36. van der Vegt, W.; van der Mei, H. C; Wösten, H. A.; Wessels, J. G. and Busscher, H. J. A.: comparison of the surface activity of the fungal hydrophobin SC3p with those of other proteins. Biophys. Chem. **57** (1996), pp. 253-260.
37. Alexandrov, N. A.; Marinova, K. G.; Gurkov, T. D.; Danov, K. D.; Kralchevsky, P. A.; Stoyanov, S. D.; Blijdenstein, T. B. J.; Arnaudov, L. N.; Pelan, E. G. and Lips, A.: Interfacial layers from the protein HFBII hydrophobin: dynamic surface tension, dilatational elasticity and relaxation times. Journal of Colloid and Interface Science. **376** (2012), no. 1, pp. 296-306.

Received 14 January 2015, accepted 18 March, 2015